Journal of Sciences, Islamic Republic of Iran 19(1): 31-48 (2008) http://jsciences.ut.ac.ir
University of Tehran, ISSN 1016-1104

A Contribution to the Genesis of Analcite after Leucite in Potassic Volcanic Rocks of the Nadik Area, Kerman, Iran

A. Moradian*

Department of Geology, Faculty of Sciences, Shahid Bahonar University, Kerman, Islamic Republic of Iran

Abstract

The origin of analcite-bearing lavas and potassic volcanic rocks is controversial in the geological record. Two main hypotheses are either primary analcite or replacement pseudomorphous of leucite. Spectacular large (5 cm) euhedral trapezohedra occur as single crystals of analcite in tephriphonolite lavas from Nadik area. Based on the following evidences the large analcite trapezohedra from Nadik area are interpreted as having formed by ion-exchange pseudomorphous replacement of primary leucite either during cooling or shortly afterwards. The absence of hydrous primary igneous minerals such as amphibole or mica, lack of evidence for rapid transport of crystals from the depths indicates the stability of the field for analcite. This indicates that primary crystallization of analcite would necessitate crystallization of a sodic pyroxene rather than diopside and preponderance of K_2O over Na_2O in bulk rock composition. Also, the homogeneous nature of the large single crystals of analcite and lack of effect on the other phases included in analcite, point out to its hydrothermal origin. The tertiary rocks from Nadik have initial $^{87}Sr/^{86}Sr$ ratios between 0.70453 and 0.70576 and the ϵNd values range from +1.3 to +4.1. Most of the potassic rocks from the Nadik show high Al_2O_3, K_2O, LFSE and LREE abundances and low abundances of TiO_2 and HFSE (Ta, Nd and Zr), in addition to LREE>Nb and Zr>Y, these features provide strong evidence of involvement of subduction-related process in the generation of orogenic analcite-bearing potassic magma in the Nadik area.

Keywords: Nadik; Potassic volcanic rocks; Tephriphonolite; Analcite; Leucite

Introduction

The origin of analcite-bearing lavas and potassic volcanic rocks is controversial in the geological record [15]. In recent years, the hydrothermal crystallization of analcite has attracted a great deal of interest, in part because of their unusual mineralogy and chemical composition. Also, the analcite-bearing potassic rocks are very important petrologically and economically. Analcite most commonly is produced during low grade metamorphism and late stage hydrothermal activity in basaltic and related rocks [38,45,54]. It occurs in veins

* Corresponding author, Tel.: +98(341)3222035, Fax: +98(341)3222035, E-mail: moradian@mail.uk.ac.ir

and cavities, as a replacement of other silicate phase and is commonly interstitial in habit. Large crystals are rare but euhedral trapezohedra up to several centimeters in size have been recorded from several occurrences of alkalic-rich undersaturrated igneous rocks variously described as phonolite, analcimite and blairmorite [65].

The origin of the analcite phenocrysts in volcanic rocks is controversial. Two main hypotheses are either primary analcite or replacement pseudomorphs of leucite [29,38,44,47]. In the last few decades, however, experimental results have turned the tide of opinion away from the concept of primary magmatic analcite. Experiments have shown that leucite, nepheline, albite, and other minerals can be rapidly converted to analcite by reaction with aqueous solutions at low temperatures [26,52]. In addition, phase-equilibrium experiments in the synthetic system $NaAlSiO_4$-$KAlSiO_4$-SiO_2-H_2O have demonstrated that analcite and silicate melt can not coexist above 650°C below about 5-Kbar pressure under water saturated conditions [32,49].

In hydrothermal experiments on a natural analcite bearing rocks from the Dippin Sill, analcite was absent above 400°C [29]. Because the crystallization temperatures of most analcite-bearing igneous rocks are thought to be much higher, euhedral analcite crystals in igneous rocks are now generally explained as low-temperature alteration products of leucite, nepheline or other precursor minerals [7,65] and in almost all known cases, analcite forms in hydrothermal conditions. In many of these occurrences, analcite is found as single crystals, a millimeter to a centimeter in size. This analcite is inferred to have been formed by dissolution of a structurally dissimilar source material for example, nepheline, plagioclase, albite or volcanic glass, and recrystallization of analcite from the hydrothermal solution. Karlsson and Clayton [32] and Giampaolo and Lombardi [22] referred it as H-type analcite. One special case of an analcite that forms under hydrothermal conditions is when the source material is the mineral leucite [38]. The framework structure of leucite is identical to that of analcite, the only difference being the cations and the H_2O content [4, 46]. Hence the leucite-analcite reaction involves an ion-exchange process: $KAlSi_2O_6 + NaCl_{aq}+H_2O = NaAlSi_2O_6, H_2O+ KCl_{aq}$. Karlsson and Clayton [31,32] and Giampaolo and Lombardi [22] call this X-type analcite, in reference to the ion-exchange character and to distinguish it from I-type or igneous analcite. They also referred to it as the secondary analcite to distinguish it from primary igneous analcite. In nature, this X-type analcite is formed as an in-situ-replacement product.

The feldespathoid-bearing rocks of central Iran have been studied by many investigators but no detailed geochemical studies have been carried out on the origin of the large crystals of analcite. Analogous large trapezohedra composed of analcite have been recorded from many areas of Iran such as Taleghan [58], Sarab, Azarbaijan [37], west Mianeh [36], south Aghda [1] and Javazm, Shahrbabak [42]. The primary or secondary origin of large analcite crystals in igneous rocks from Nadik has been the topic of debate, for a considerable time and is discussed in more detail below.

Geological Setting

The analcite-bearing potassic igneous rocks from the Nadik area in the Urumiyeh-Dokhtar Volcanic Belt (U-DVB) are located in the middle of the extensive Alpine-Himalayan orogenic belt between the Arabian and Eurasian plates. The Nadik area is located in the Southeastern part of the U-DVB and in the Shahrbabak, South-Southwestern Kerman province, Iran on latitude 30° 24′ N and longitude 55° 06′ E (Fig. 1). The tectonomagmatic model of the U-DVB has been controversial. The most popular model, however involves Andean type subduction of the Tethyan oceanic crust beneath the central Iran plate during the Tertiary to generate the volcanism [3,21].

Analcite-bearing volcanic rocks occur in the Hezar complex from the Dehaj-Sarduieyeh Belt where a sequence of basaltic, andesitic and trachytic lavas with pyroclastic units and associated sedimentary strata are developed. The Hezar series where the Nadik area is located in it is undersaturated K-rich units which form the basis for the present investigation. Volcanism and accompanying intrusive activity in the general region continued until the Pliocene [2]. The Hezar series described by Sardic [55] and Dimitrijeovice [12] and forms the upper part of the Eocene volcanic sequence. It covers a large part of the Nadik study area (Fig. 1). The succession comprises a series of mainly tephriphonolite, basalt, trachybasalt, trachyandesite lavas and dacite with a few pyroclastic units. Volcanic units of these series lack biotite and amphibole but are characterized by the occurrence of large analcite pseudomorphous after leucite set in a groundmass rich in K-feldspar (Table 1).

Analcite crystals occur in three stratigraphically adjacent tephriphonolite lava flows, which overlie about 20 m of red tuff. Small analcite crystals are restricted to the lower flow and large trapezohedra are restricted to the middle and upper flows.

Analcite crystals display a euhedral, cubic trapezohedral form (Fig. 2A) and may comprise up to approximately 35% of the host rocks. During weathering, trapezohedra released from the lavas are concentrated on the tops and beside of these units. In

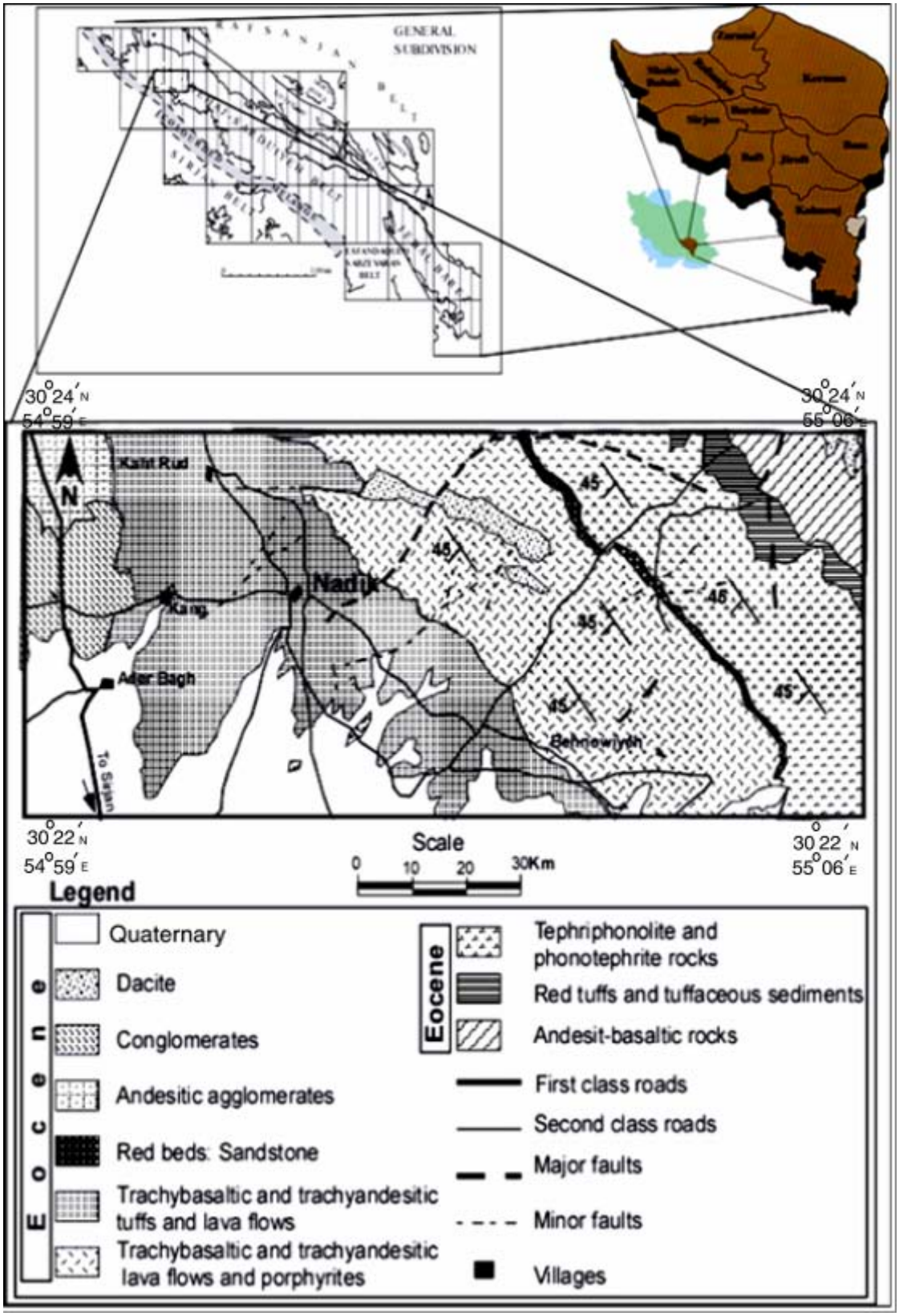

Figure 1. Geological map of Nadik area, after Sardic *et al.* [55].

Table 1. Modal data for analysed samples of Eocene potassic rocks of Nadik area

	TP			B	TB	TA	D
Phenocrysts	Mean(8)	Range	Size mm	Mean(4)	Mean(5)	Mean(6)	Mean(3)
Diopside	2.10	0.5-2.4	1.0-2.3	5.3	3.0	3.3	
Plagioclase	10.02	7.5-15.3	1.2-5.9	16.7	18.9	10.3	21.5
Sanidine	10.3	5.3-21.5	2.0-5.2	7.5	4.5	21.0	3.9
Nepheline							
Analsime	35.0	23.0-39.0	5.0-50.0				
Olivine				4.0	3.3		
Hornblende						1.7	
Quartz							4.52
Biotite							3.9
GROUNDMASS							
Diopside	2.2	0.3-4.2	0.3-0.6	16.0	4.5		
Plagioclase				40.6	52.8	42.5	31.8
Sanidin	34.0					2.8	5.7
Hornblend							4.9
Biotite							1.5
Fe-Ti Oxide	2.1			6.6	7.0	5.4	
Quartz							13.0
Others	3.2			3.3	6.0	13.0	4.5

Others: Calcite, cholorite, apatite, serisite, epidot and zeolite,
TP=tephriphonolite, B=basalt, TB=trachybasalt, TA=trachyandesite, D=dacite and T=trachyte

addition to the large analcite, the lavas also contain phenocrysts of plagioclase, K-feldspar, nepheline and clinopyroxene. Primary groundmass minerals comprise plagioclase, K-feldspar, nepheline, clinopyroxene, Fe-Ti oxide and apatite.

According to Hassanzadeh [28] and based on ^{40}Ar-^{39}Ar and Rb-Sr isotopic age dating, the age of crystallization is approximately 29 Ma.

Analytical Techniques

Major and most trace element were determined by X-ray fluorescence (XRF) spectrometry using automated Phillips PW 1450 spectrometer at the Australian National University, Australia by professor Bruce Chappell following the methods of Norish and Chappell. REE, U, Th, Hf, Sc and Ta were determined on 5 representative samples by instrumental neutron activation method (INAA) at Bequerel Laboratories by Dr David Garnett. Mineral compositions were determined on polished thin section. The analyses were performed using a fully automated, Cameca SX50 electron microprobe (Maquari University and the Australian National University), calibrated with natural mineral standards. Analytical conditions were set at an accelerating voltage of 15 Kv and beam current of 20 nA.

A representative subset of 5 whole rock powders was analyzed for strontium and neodymium isotopic ratios at Australian CSIRO. $^{87}Sr/^{86}Sr$ and $^{143}Nd/^{144}Nd$ were measured on a VG 54E mass spectrometer and were normalized to $^{86}Sr/^{88}Sr = 0.1194$ and $^{146}Nd/^{144}Nd = 0.7219$ respectively. Replicate analyses of NBSSRM 98 gave $^{87}Sr/^{86}Sr = 0.710251\pm 28$ (external precision at 2σ, n = 17) and the JM-Nd standard gave $^{143}Nd/^{144}Nd = 0.51111+12$ (external precision at 2σ, n = 17).

Petrography

The Eocene volcanic rocks from the Nadik area are composed of tephriphonolite, basalt, trachybasalt, trachyandesite and dacite. These lithologies occur as lavas, plugs, dykes and pyroclastic breccia. Petrographic data of the Nadik volcanic rocks is summarized in Table 1. Five different rock types which occur in the Nadik region have common mineralogical characteristics. The exception is the tephriphonolite lavas which contains abundant of large trapezohedra of analcite. All samples are porphyritic with a holocrystalline groundmass.

Tephriphonolite rocks are brownish in colour. Samples consist of phenocrysts of diopside, sanidine, plagioclase, nepheline and abundant analcite which originated by pseudomorphs replacement of primary leucite. The groundmass is holocrystalline and fine-grained.

The phenocrysts of diopside are euhedral to subhedral grains with a maximum dimension of 2.4 mm. Some grains have ragged edges due to resorption and most show minor compositional zoning and have inclusions of titanomagnetite and apatite.

Sanidine is the most abundant phase in the tephriphonolite rocks and occurs both as euhedral phenocrysts up to 5mm long and as abundant, small lathe in the groundmass. Most phenocrysts show at least partial alteration to kaolinite and sericite and commonly contain inclusions of titanomagnetite and apatite.

Plagioclase occurs as euhedral to subhedral phenocrysts between 1.2 and 5.9 mm long. Twinning according to the albite and albite-carlsbad law is common and thin rims of sanidine occur on many phenocrysts.

Analcite occurs as abundant trapezohedra between 5.0 and 50.0 mm in size and are brownish and pinkish in colour. These trapezohedra differ in size0 and abundance throughout the study area. Collectively, the large crystals may comprise up to 35% of the host unite and all crystals contain abundant inclusions of plagioclase, pyroxene and titanomagnetite. Some analcite trapezohedra show a relict complex twinning. The leucite-analcite transformation is accompanied by a 10% volume increase [31]. If the mineral transformation occurred after the magma had solidified, as has been maintained here, then some expansion cracks could have resulted. Figure 2C shows that cracks are present in some samples.

The mineralogy of other rock samples comprises plagioclase, sanidine, pyroxene, hornblende, biotite, olivine and titanomagnetite, together with accessory apatite and zircon. Quartz phenocrysts in samples of dacite are embayed as a result of resorption. Fresh olivine occurs in basalt and trachybasalt, but this mineral is almost invariably replaced by one or more of a variety of secondary minerals including chlorite and iddingsite. Plagioclase is the dominant felsic mineral in most rock types and occurs as euhedral to subhedral phenocrysts between 1.2 and 5.8 mm long. Normal and oscillatory zoning are common (section plagioclase) as is albite and carlsbad twinning and alteration to sericite.

Based on microprobe analysis, the composition of plagioclase phenocrysts ranges from oligoclase to bytownite (Table 3, Fig. 4a). Some phenocrysts contain titanomagnetite inclusions and grains are generally fresh although a few exhibit minor alterations to sericite. Sanidine is the only K-feldespar present in samples from the Nadik area and it is a major constituent of trachyandesite, phonotephrite and tephriphonplite samples.

Diopside is the only pyroxene, present in samples from the Nadik area. Euhedral to subhedral diopside crystals show simple twinning and inclusions of titanomagnetite and apatite. Anhedral grains of titanomagnetite occur in the groundmass and as inclusion in other minerals. Hornblende, biotite and Fe-Ti oxides are the only mafic minerals in dacite.

Biotite grains are euhedral to anhedral in shape and occur as brownish phenocrysts and in the groundmass. Some grains are corroded and many show alteration to cholorite and opaques.

Secondary mineral including calcite, zeolite, kaoline, cholorite and epidote comprise about 4.5% of the total rock volume.

Mineral Chemistry

Average phenocryst compositions for analcite, plagioclase, sanidine, pyroxene and Fe-Ti-oxides from different rock types are summarized and discussed in the following sections.

Analcite

Analcite is a cubic, hydrated Na-aluminosilicate mineral and occurs as a primary and secondary mineral in alkaline rocks. The analcites of the Nadik are euhedral and up to 5 cm in diameter. The chemical composition of the majority of natural analcite is remarkably constant, the only appreciable variation being in the partial replacement of sodium by minor amounts of potassium or calcium, and in the substitution of Al for Si, which necessitates an increase in the (2Ca +Na +K) ions to maintain the charge balance [10]. Large analcite phenocrysts variously suggested as being of primary igneous origin or due to transformation from original leucite by Na-exchanged leucite [30].

Representative analyses of analcite from Nadik are presented in Table 2. The analcite trapezoherdra are remarkably homogeneous (Table 2, Fig. 3b), with chemical variation being within analytical uncertainty associated with electron microprobe analyses. However, the lava may have first cooled rapidly by several hundred degrees and then cooled at a slow rate. Thus, there could have been sufficient time to allow the leucite-analcite transformation to go to completion [31]. Taylor and Mackenzie [60] demonstrated experiment-tally that this transformation can occur during cooling.

It seems likely that analcite, when formed at high temperature have strictly cubic symmetry, but by cooling they invert to a tetragonal or trigonal (Pseudocubic) modification [8]. Pearce [49] also points out that the analcite occurs in a variety of different color, including brown, red, orange and green, the brown analcite, he asserted, is the unaltered original mineral, whereas the other colored varieties are alteration products. Ferguson and Edgare [19], suggested that the color variation may be due to nothing more than the presence or absence of various inclusions. The petrography and field relations of the Nadik volcanic both support a secondary origin for analcite in these rocks. The analyses of tephriphonolite samples were calculated to 100% and recalculated in terms of nepheline, kalsilite and quartz and plotted in the Ne-Ks-Qz diagram (Fig. 3a). Figure 3a shows that the samples from Nadik area are plotted in the feldspar field between 780°C and 850°C.

A

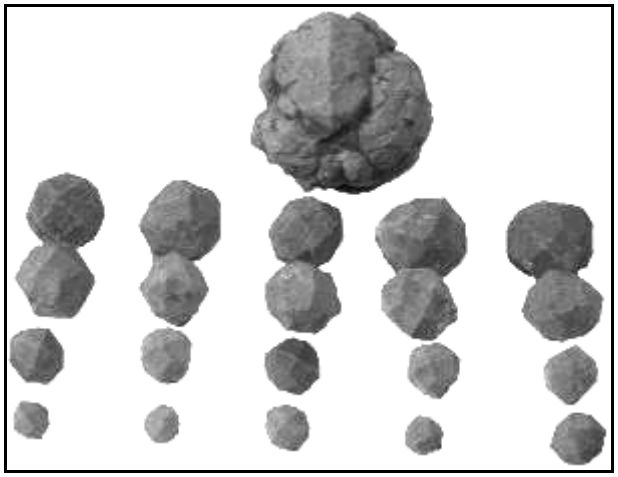

B

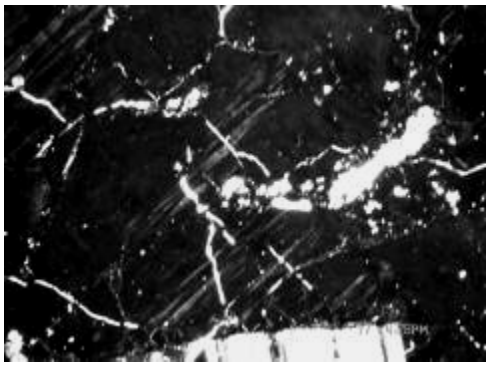

C

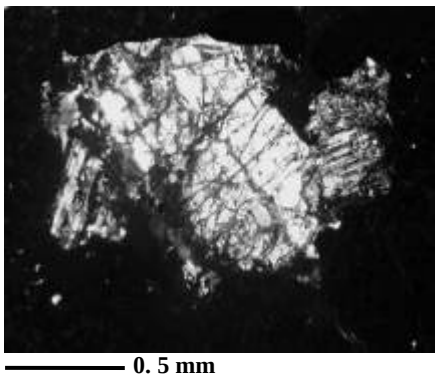

Figure 2. A, Euhedral trapezohedral of analcite; B, Photograph of multiple twin lamella and C; cracks in inclusion of analcite in thin section (XPL).

A

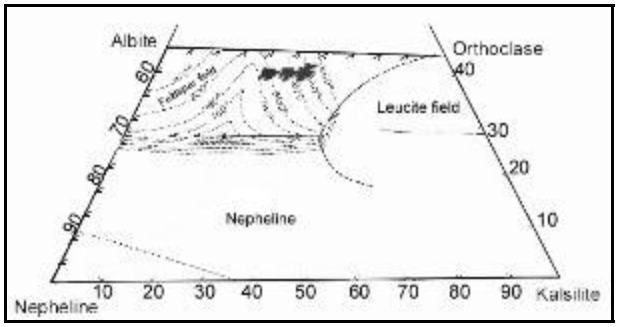

B

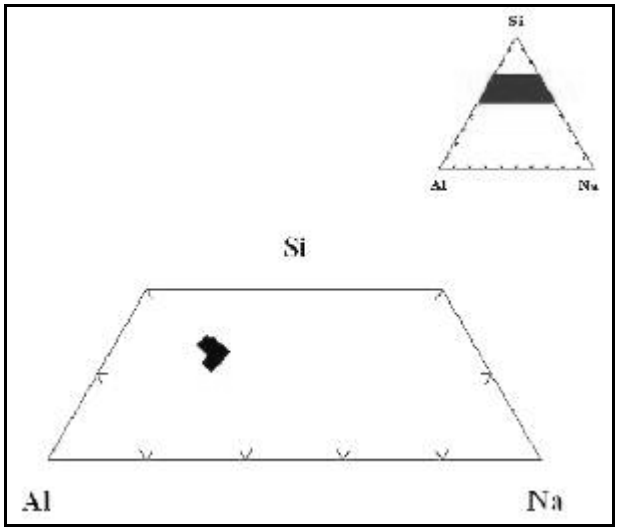

Figure 3. A, plot of the chemical composition of analcite-bearing rocks of Nadik in the system nepheline-kalsilite-SiO_2 at different temperatures under 2Kb PH_2O, after Taylor and Mackenzie [60]. B, Electron-microprobe composition of analcites from the Nadik in Si, Al, Na diagram. Data are in mol% Si, Al, Na.

Table 2. Mineral chemistry of analcite in tephriphonolite from Nadik area

sample	N142	N145	N147	N142	N145	N145	N148	N147
SiO2	61.37	60.49	60.85	61.84	60.07	60.50	61.88	59.85
TiO2	0.07	0.04	0.06	0.05	0.02	0.03	0.08	0.11
Al2O3	23.14	23.24	22.53	23.49	24.01	23.98	22.80	22.77
CaO	0.04	0.06	0.09	0.05	0.06	0.05	0.13	0.38
MnO	0.00	0.00	0.04	0.02	0.02	0.01	0.02	0.05
FeO	0.35	0.27	0.27	0.36	0.23	0.24	0.32	0.78
Na2O	5.67	6.70	6.10	6.16	6.70	6.73	6.23	6.84
K2O	0.08	0.04	0.03	0.12	0.05	0.05	0.03	0.03
Total	90.72	90.84	90.09	92.11	91.16	91.49	91.52	90.81
Si	28.68	28.27	28.44	28.90	28.08	28.20	28.92	27.94
Ti	0.04	0.02	0.04	0.03	0.01	0.02	0.05	0.07
Al	12.25	12.30	11.93	12.43	12.71	12.69	12.45	11.65
Ca	0.03	0.04	0.06	0.04	0.04	0.03	0.11	0.34
Mn	0.00	0.00	0.01	0.01	0.02	0.01	0.01	0.03
Fe	0.27	0.21	0.21	0.28	0.18	0.19	0.25	0.71
Na	4.21	4.97	4.53	4.58	4.97	4.98	4.61	5.02
K	0.07	0.04	0.03	0.10	0.04	0.04	0.02	0.03

Table 3. Representative analysis of plagioclase from potassic rocks of the Nadik area (C = Core, R = Rim)

z	T		B		TB		TA		D	
Wt%	C(12)	R(4)	C(4)	R(3)	C(5)	R(5)	C(4)	R(4)	C(3)	R(4)
SiO2	53.50	67.95	45.94	53.50	57.50	57.30	60.00	63.20	60.50	61.00
TiO2	0.07	0.07	0.04	0.05	0.15	0.15	0.05	0.06	0.03	0.01
Al2O3	28.15	20.20	33.00	26.00	26.20	25.50	26.80	22.85	24.15	23.80
MgO	0.00	0.00	0.00	0.18	0.00	0.00	0.00	0.00	0.00	0.00
CaO	11.25	1.05	17.50	9.00	7.50	8.45	9.60	4.40	5.90	5.50
FeO	0.55	0.15	0.80	0.95	1.00	0.80	0.44	0.30	0.15	0.16
Na2O	4.65	9.60	1.85	3.95	6.25	6.20	5.40	8.20	7.95	8.15
K2O	0.75	1.50	0.15	0.25	1.50	1.15	1.15	1.12	0.70	0.65
An	54.31	5.07	83.15	57.50	36.30	39.6	46.30	21.25	28.00	26.30
Ab	41.30	86.50	16.30	17.75	55.20	54.65	47.15	72.40	68.65	70.15
Or	4.25	8.20	0.72	1.35	8.60	6.00	6.65	6.50	3.50	3.65

Plagioclase

Plagioclase is the dominant felsic mineral in most rock types. The mean composition of plagioclase grains are shown in Table 3. Most plagioclase phenocrysts from the Nadik region have Ca-rich cores and more Na-rich rims (Table 3, Fig. 4a), which is attributed to normal magmatic fractionation. Most plagioclase crystals show an increase in Na_2O and decrease in Al_2O_3 with increasing SiO_2 content (Table 3, Fig. 4b). Plagioclase phenocrysts in some tephriphonolite samples are commonly rimmed by sanidine. This mantling of plagioclase by sanidine may occur due to a shift in composition and temperature of the magma in either the magma chamber or during ascent from the chamber to the surface.

Some plagioclase phenocrysts in tephriphonolite rocks show minor normal compositional zoning with the

A

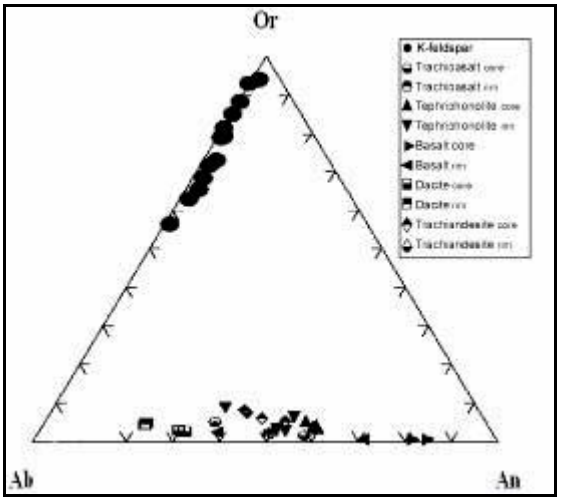

B1

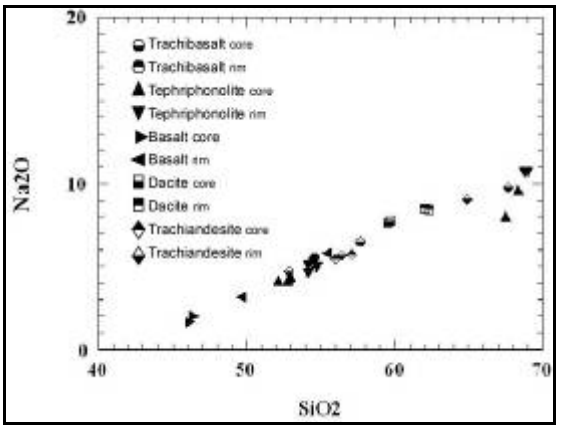

B2

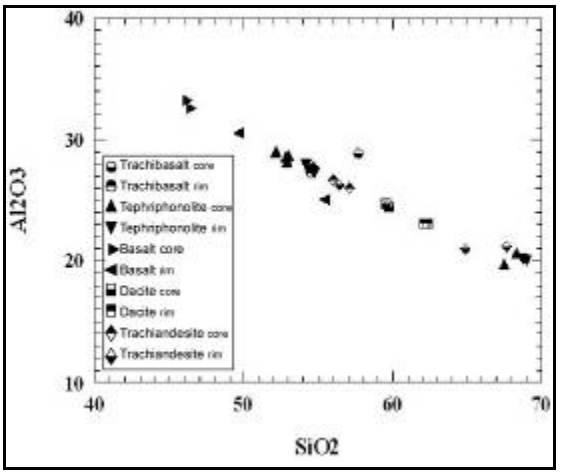

Figure 4. A, Feldspar composition for samples from Nadik; B1 and B2, variation of SiO_2 with Na_2O and Al_2O_3 in plagioclases from Nadik.

exception of plagioclase in the dacite, which show oscillatory zoning in thin section. These oscillatory zoned grains have a compositional range from cores of An31.5 to rims An22.1. Zoning in plagioclase is indicative of failure of mineral to attain equilibrium with the surrounding liquid and is normally attributed to change in temperature and pressure either within the magma chamber or during ascent from the chamber to the vent [40]. Oscillatory zoning in plagioclase is hiatal or episodic in nature. It is probably due to pulses of growth alternating with periods of dissolution, reaction or lack of growth (possibly very slow growth). The growth is therefore periodic but discontinuous [47,57].

The composition of plagioclase phenocrysts in tephriphonolite from Nadik are labradorite (An50.83 to An59.2, Table 3). Plagioclase phenocrysts in tephriphonolite from study area, however, have more sodic rims than plagioclase in all other rock types (Table 3). Plagioclase crystals in basalt and trachybasalt from Nadik range from oligoclase to bytownite (An18.7 to An84.1) in composition (Fig. 4a). Compositions of cores and rims of plagioclase phenocrysts in dacite do not show any appreciable variation and have overall range from oligoclase to andesine (An 21.8 to An 31.5) (Fig. 4a). The average contents of TiO_2, Al_2O_3, FeO and K_2O, however are slightly higher in trachyandesite than dacite.

K-Feldspar

Sanidine is the only K-feldspar present in tephriphonolite and trachyandesite from the Nadik area. The average composition of sanidine Phenocrysts in tephriphonolite and trachyandesite are given in Table 4. The amount of TiO_2 and MgO in the samples from the study area is very low, while FeO ranges from 0.15 to 0.18. CaO is usually less than 1% but it is greater in the trachyandesitic rocks (Table 4). The sanidine Phenocrysts have a compositional range of Or75.90 to Or78.20 in tephriphonolite and trachyandesite (Table 4, Fig. 4a), similar to the K-feldspar from central Italy [50]. The high-potassic sanidine crystals are associated with the high-calcic plagioclase in the tephriphonolite from the Nadik area.

Pyroxene

Diopside is the only pyroxene present in samples from Nadik area (Fig. 5). The mean composition of diopside phenocrysts in samples from study area are shown in Table 4. In most diopside crystals, the average MgO content is higher in the core than the rim; where as the average FeO content is lower in the core than the

Table 4. Chemical data for pyroxene and sanidine and titanomagnetite in potassic rocks of the Nadik area

Wt%	Pyroxene					Sanidie		Fe-Ti oxides
	TP		*B*	*TB*		*TP*	*TA*	*TP*
	C(9)	R(8)	Mean(5)	C(6)	R(6)	Mean(14)	Mean(5)	Mean(8)
SiO2	49.50	50.20	47.02	51.00	49.00	65.00	65.20	0.95
TiO2	0.95	0.92	1.15	0.80	1.08	0.05	0.02	17.36
Al2O3	3.15	2.90	6.53	4.00	4.90	19.05	18.30	1.30
MgO	12.85	12.50	12.95	15.50	13.70	0.06	0.03	0.07
CaO	22.55	22.05	21.85	22.00	21.95	0.50	0.15	0.45
MnO	0.38	0.42	0.35	0.19	0.25	0.03	0.02	2.00
FeO	9.30	9.95	8.73	5.80	7.50	0.15	0.18	69.72
Na2O	0.51	0.54	0.53	0.45	0.70	2.45	2.30	0.03
K2O	0.02	0.03	0.02	0.01	0.02	12.95	13.20	0.05
Wo	46.95	46.65	46.47	45.85	46.70			
En	38.06	37.25	38.82	44.65	40.65			
Fs	4.60	17.00	14.87	9.60	12.80			
An						2.40	0.60	
Ab						21.65	21.20	
Or						75.90	78.20	

rim (Table 4). This enrichment of FeO from core to rim is consistent with normal fractionation during magmatic evolution. Diopside Phenocrysts in tephriphonolite and trachybasalt from the Nadik range from WO47.8 En38.8 Fs13.4 to WO 45.6 En 35.7 Fs 18.7 and from WO46.9 En 44.8 Fs 8.3 to WO 47.9 En 32.7 Fs 19.4 in composition, respectively (Fig. 5). In trachybasalt, the mean MgO and CaO contents of phenocrysts decrease from core to rim, whereas TiO_2, Al_2O_3, FeO and Na_2O increase. Rims are relatively enriched in ferrosilite compared with the cores (Table 4). Titanomgnetite grains in tephriphonolite from study area have the lowest MgO content compared with all other samples (Table 4). Titanomagnetite grains in tephriphonolite from study area are compositionally similar to titanomagnetite crystals in the tephrite and phenol-tephrite from eastern Paraguay [15] and the Roman province, Italy [9]. Other minerals include olivine, amphibole and biotite.

Geochemistry

Major and Trace Element Data

The mean and range of compositions for representative analyses of major and trace elements, REE and Sr and Nd ratios for Nadik Tertiary analcite-bearing potassic rocks listed in Tables 5 and 6. Based on the IUGS recommendation with regards to the nomenclature of igneous rocks [35], these extrusive rocks are subdivided into tephriphonolite, basalt, trachybasalt, trachyandesite and dacite. The chemical analyses of samples from the study area have been plotted on the K_2O versus SiO_2 diagram [35,53]. Figure 6 shows that for the Nadik area, all samples belong to three series comprising shoshonitic, high-K calcalkaline and calcalkaline rocks.

Most of the analysed rocks from Nadik belong to the mafic-intermediate group which, on average, contains higher contents of TiO_2, Fe_2O_3, MgO, CaO, Al_2O_3, P_2O_5 and incompatible elements and lower TiO_2, Fe_2O_3, MgO and CaO than the felsic and mafic group, respectively (Tables 5 and 6).

The SiO_2 content shows large variation from 47.73 Wt% in basalt to 66.60 Wt% in dacite, also the TiO_2 content decreases from mafic to felsic rocks reflecting the higher modal titanomagnetite in mafic rocks, (Tables 5 and 6).

The content of Al_2O_3 is relatively high and variable (15.20 to 20.4 wt%, Tables 5 and 6). Although the Al_2O_3 content is higher in tephriphonolite than the other samples, and reflects the higher modal abundance of an-

alcite and K-feldspar in these rocks (Tables 1, 5 and 6).

The high MgO value for trachybasalt is related to the higher modal olivine in this sample [18]. The content of CaO in basalt is higher than the other rocks probably either related to the higher modal clinopyroxene or plagioclase in these rocks (Tables 5 and 6). The average content of Na_2O is higher than K_2O in the rocks from Nadik except tephriphonolite rocks (Tables 5 and 6). The trachybasalt show the maximum Mg-value (71.90) for analyzed samples from Nadik, and the majority of samples have Mg-value in the range of 23-59.6 and only one sample has a Mg-value of more than 70. The low Mg-value, Cr and Ni contents in these mafic rocks preclude their being primary melts of mantle periodotite [56]. The average content of SiO_2 and TiO_2 is lower and the Al_2O_3, Fe_2O_3, MgO and K_2O high in tephriphonolite rocks compared to the trachyandesite rocks from the study area (Tables 5 & 6) reflecting more abundances of analcite and sanidine in tephriphonolite rocks (Table 1).

In mafic-intermediate rocks the content of Y increases from trachybasalt towards the trachyandesite, and reflects the presence of apatite and zircon in trachyandesite. Niobium concentration is up to 14 ppm in different rock types of Nadik and is highest in trachyandesite (Tables 5 and 6). Trachyandesite and basalt from Nadik area have the highest (410 ppm) and the lowest (66ppm) contents of Zr respectively (Tables 5 and 6).

Comparison of major element geochemical data for shoshonitic rocks with more than 52% SiO_2 from many region (Table 5) shows that these rocks form a coherent group and that data for Nadik rocks lie within the range of values for all regions. The exception being K_2O and Al_2O_3 which are higher than all other oxides (Table 5). The Fe_2O_3 values for shoshonitic rocks from the Abitibi Greenstone Belt [14], (Table 5, column C) are higher than other regions. Rocks from Northwest Alp, Italy [64], (Table 5, column B) have higher TiO_2, MnO, MgO and CaO and lower P_2O_5 and K_2O than similar rocks from elsewhere. The shoshonitic rocks from Nadik have higher contents of Ba, Rb, Th, U and Zr while rocks from the Abitibi Greenstone Belt have lower U, Tb and Ce than similar rocks from elsewhere. The rocks from Nadik contain higher contents of HREE (Yb and Lu), MREE (Sm and Eu) and LREE (La and Ce) than the Northwest Alps, Italy, while the LREE (La and Ce) and MREE (Sm and Eu) contents of sample from the Abitibi Greenstone Belt are higher than the other regions.

Rare Earth Elements

The REE concentrations for samples of tephriphonolite, basalt, trachybasalt and trachyandesite from Nadik are plotted relative to chondrite in Figure 7. The REE patterns for the tephriphonolites and the trachyandesite of Nadik are similar, except that the trachyandesite is more enriched in HREE. These rocks are strongly fractionated in LREE and relatively have a flat MREE to HREE pattern (La_N/Yb_N values of 6.62 to 7.98), with moderate to strong negative Eu anomalies (Eu/Eu* = 0.61 to 0.79). Negative Eu anomalies are normally interpreted as resulting from removal of plagioclase or may be due to decreasing oxygen fugacity [27].

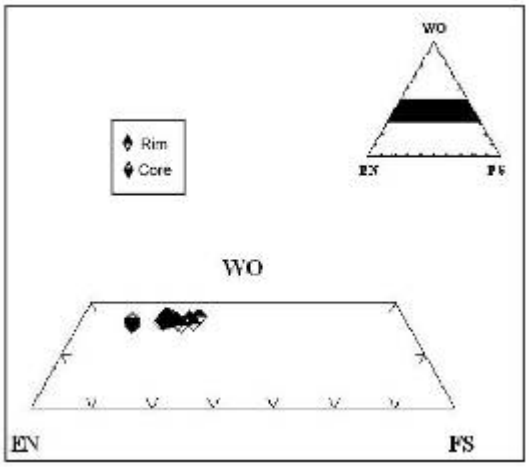

Figure 5. Compositions of diopside phenocrysts for rocks from Nadik.

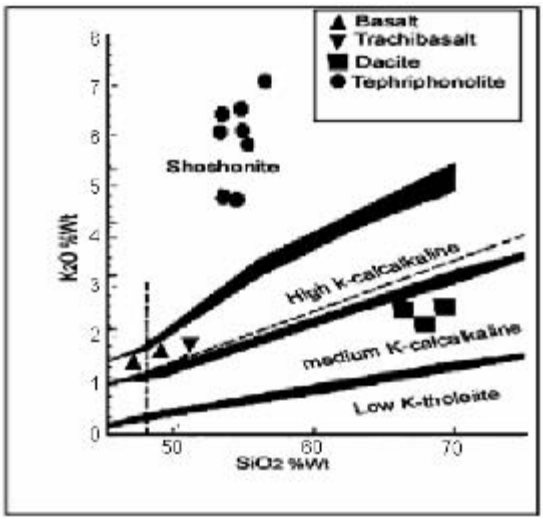

Figure 6. K_2O versus SiO_2 diagram for volcanic rocks from Nadik, after Le maiter *et al.*, [35] and Rickwood [53].

Table 5. Whol-rock geochemical for tephriphonolite from Nadik (A), Northwest Alp, Italy(B), Abitibi Greenstone Belt (C) and Azarbaijan(D), (oxides, Wt% and trace PPm)

Sample	**A**								**B**	**C**	**D**
	N142	*N152*	*N154*	*N157*	*N158*	*N142*	*N160*	*N148*			
SiO_2	54.60	54.82	53.18	54.35	54.40	53.25	55.19	53.40	53.11	54.74	55.51
TiO_2	0.87	0.75	0.82	0.80	0.65	0.76	0.68	0.85	1.11	1.09	0.72
Al_2O_3	18.40	19.24	19.12	19.15	19.35	19.25	20.04	19.60	17.21	16.61	18.30
Fe_2O_3	6.45	5.30	6.20	5.80	4.20	6.05	4.90	6.03	8	8.77	4.48
MnO	0.15	0.16	0.14	0.10	0.14	0.13	0.13	0.12	0.16	0.12	0.11
MgO	1.63	1.41	1.95	2.30	0.95	1.57	1.90	2	4.96	3.61	0.98
CaO	4.20	3.65	4.85	4.11	2.78	4.25	3.42	4.60	6.83	4.91	5.23
Na_2O	4.15	5.01	4.10	5.40	4.85	4.20	5.00	5.06	2.46	3.32	5.01
K_2O	6.45	6.06	6.05	4.70	7.05	6.42	5.80	4.77	2.65	3.18	5.30
P_2O_5	0.56	0.34	0.43	0.38	0.26	0.46	0.35	0.46	0.27	0.51	0.43
LOI	3.11	3.50	3.50	3.60	3.96	4.16	3.70	3.33	3.11	1.71	
Total	100.47	100.20	100.22	100.45	100.27	100.31	100.80	100.18			
Ba	1300	1262	1210	1115	1065	1210	1315	1132		745	
Rb	172	230	205	152	385	187	160	120	90	97	
Sr	480	662	682	610	550	641	786	815	521	611	
Th	17	18.01	18	17	19	19	17.50	16	6.19	7.92	
U	3	6	6	4	5	4	4	4.06	2.51	1.92	
Zr	206	195	193	174	204	174	175	193	120	187	
Nb	9	11	10	10	10	10	10	10	11	15.21	
Y	25	24	26	24	23	23.05	22	24	31	24.05	
La	33.21	32	30	29	30	30	29.50	29.85	22.71	52	
Ce	64.55	62	64	64	65	64.88	60	59.85	44.11	116	
Nd	31.50							29.75	24.31	54.21	
Sm	6.45							5.94	5.21	8.51	
Eu	1.52							1.52	1.43	1.91	
Tb	0.93							0.80	0.81	0.78	
Ho	1.23							0.99			
Yb	2.80							2.53	2.51	2.22	
Lu	0.42							0.38	0.36	0.33	
Sc	7.60							7.77		18	
V	88	83	81	103	40	82.02	70	117	205	137	
Cr	<1	4.01	6.02	22	<2	4	4	5	77	100	
Ni	2	4	6	16	<2	4	4	9	25	31	
Zn	72	70	68	78	50	78	54	69			
Sn		<5	<5	<5	<5	<5	<5				
Ga	16.45	18	17	18	18	18	17	18			
Hf	3.70							3.69	3.18	4.37	
Ta	0.67							0.67	0.53	0.68	
REE∑	142.55							131.56			
Eu/Eu*	0.71										
La_N/Yb_N	7.99						7.88				
$^{87}Sr/^{86}Sr$	0.70565							0.70520			
$^{143}Nd/^{144}Nd$	0.51267							0.51275			

Table 6. Average whole-rock geochemical data for trachybasalt, trachyandesite and dacite from Nadik (Oxides, Wt% and trace, PPm). B = Basalt, TB = trachybasalt, TA = trachyandesite and D = Dacite

Sample	**B**	**TB**	**TA**			**D**		
	Min			Rang			Rang	
			Mean	*Minimum*	*Maximum*	*Mean*	*Minimum*	*Maximum*
SiO_2	47.73	50.05	59.13	58.60	59.65	66.60	65.40	67.65
TiO_2	1.05	0.98	0.81	0.68	0.95	0.42	0.35	0.46
Al_2O_3	18.02	15.20	18.06	17.70	18.43	16.25	15.55	17.70
Fe_2O_3	10.45	8.40	5.32	4.94	5.70	2.65	1.98	3.25
MnO	0.20	0.16	0.08	0.07	0.09	0.03	0.02	0.05
MgO	5.65	8.50	1.45	1.25	1.65	0.75	0.25	1.15
CaO	9.43	9.50	3.93	2.40	4.25	3.65	2.20	4.40
Na_2O	2.95	3.90	4.76	3.83	5.69	4.30	4.00	4.60
K_2O	1.58	1.55	4.62	4.20	5.04	2.50	2.25	2.70
P_2O_5	0.32	0.58	0.31	0.25	0.37	0.18	0.15	0.20
LOI	3.35	0.90	1.95	1.86	2.03	2.60	1.55	3.50
Total	100.73	99.67	99.60	95.16	104.03	99.93	93.7	105.66
Ba	538	805	420	315	525	715	518	825
Rb	50	30	140	114	166	65	56	70
Sr	605	1353	490	410	570	675	610	840
Pb	5	8	16	14	18	12	10	16
Th	2	9	20	16	24	9	7	12
U	75	2	5	4	6	3	2	4
Zr	2	118	370	330	410	140	132	154
Nb	20	12	13	12	14	7	5	9
Y	15.35	18/	32	30	34	13	7	30
La	35.00	42.00	35.00	34.00	36.00	25.40	16.00	33.00
Ce	18.50	90.00	74.50	74.00	75.00	49.50	35.00	65.00
Nd	4.40		33.50			19.80		
Sm	1.40		66.76			3.45		
Eu	0.70		1.32			0.83		
Tb	0.80		0.96			0.38		
Ho	1.81		1.40			0.40		
Yb	0.30		3.60			0.61		
Lu	8.40		0.58			0.09		
Sc	263		8.25			4.20		
V	60	175	112	63	161	50	43	68
Cr	48	328	4	3	5	19	6	43
Ni	75	160	4	4	4	8	4	12
Zn	18	75	68	59	77	42	24	55
Ga	1.66	19	16	12	20	18	17	20
Hf	0.50		8.50			3.65		
Ta	78.26		0.95			0.95		
REE	7.45		157.62			100.46		
La_N/Yb_N	0.96		6.62			32.53		
Eu/Eu	36.00		0.61			0.75		
DI	57.00	40.12	74	68	80	76.50	72.50	81
Mg≠	0.70540	71.90	40	35.40	44.60	38	23	46.50
$^{87}Sr/^{86}Sr$	0.51272		0.70474			0.70453		
$^{143}Nd/^{144}Nd$	1.8		0.51274			0.51282		
ϵNd			3.0			4.1		

Basalt is characterized by a lower enrichment in LREE compared with other samples and unfractionation for HREE (Fig. 7), with a La_N/Yb_N ratio of 7.45, implying that it is unrelated to the other rocks. One sample of dacite display similar pattern and have the most fractionated REE pattern compared with other samples with La_N/yb_N ratios 32.53. However, this sample appears to be genetically unrelated to other rocks from Nadik area. The high La_N/Yb_N ratios, suggest an important role for clinopyroxene in their formation, because partition coefficient of HREE are higher than the LREE in clinopyroxene [25]. The REE contents for the Nadik rocks are higher than those of Abitibi Greenston Belt rocks [14], and are lower than those of Colorado rocks [61].

Sr and Nd Isotopes

As shown in Tables 5 and 6, the Tertiary rocks from Nadik area have initial $^{87}Sr/^{86}Sr$ ratios between 0.70453 and 0.70567 and the ϵNd values range from +1.3 to +4.1. The range of initial isotopic values for the analysed samples is significantly higher than the estimated 2σ analytical uncertainty which equate to ± 0.00005 and ± 0.5 for initial $^{87}Sr/^{86}Sr$ and ϵNd units respectively. The samples of tephriphonolite have the highest initial $^{87}Sr/^{86}Sr$ ratio, and the lowest ϵNd (+1.3) compared with samples from the Nadik area. The felsic rocks (dacite) have the low initial $^{87}Sr/^{86}Sr$ ratio (0.70453). Figure 8 shows the relationship of the Sr isotopic data with SiO_2. The Sr isotopic data show a negative correlation from mafic to felsic rocks relative to SiO_2 (Fig. 8). Due to negative correlation of Sr isotopic value from mafic to felsic rocks of the Nadik region, these rocks can not be genetically related. However, isotope variability in mafic rocks is not related to a simple fractionation processes, because the range of initial isotopic values is higher than the analytical uncertainty.

Discussion

The origin of analcite in potassic volcanic rocks has been of growing importance. Despite the large volume of research, aspects of mineralogy, geochemistry and interrelationship of coexisting minerals have remained poorly understood. Although analcite is relatively common in some alkaline igneous rocks, only rarely does it form euhedral crystals, indicating its probable crystallization from a liquid. It is most spectacular development as a primary phase is probably in blairmorites, which have been described from only two localities: the Crowsnest formation in Alberta, Canada, and the Lupata gorge, Mozambique [67] and in the Colima minettes [39]. The most likely rock types to contain primary igneous analcite are lamprophyres and minettes. These are mafic alkalic dikes, containing phenocrysts of Mg-mica or amphibole and biotite and groundmass feldspars [66]. Some petrographers have interpreted euhedral phenocrysts or microphenocrysts of analcite in mafic alkalic igneous rocks as primary crystals that crystallized directly from a silicate melt [48,64]. Pearce [48,49] attributed the origin of the analcite-bearing volcanic rocks in the Crowsnest to

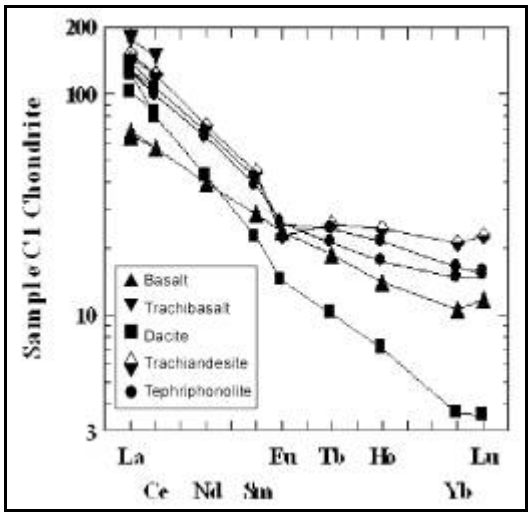

Figure 7. Chondrite-normalised rare-earth element data for samples of Nadik.

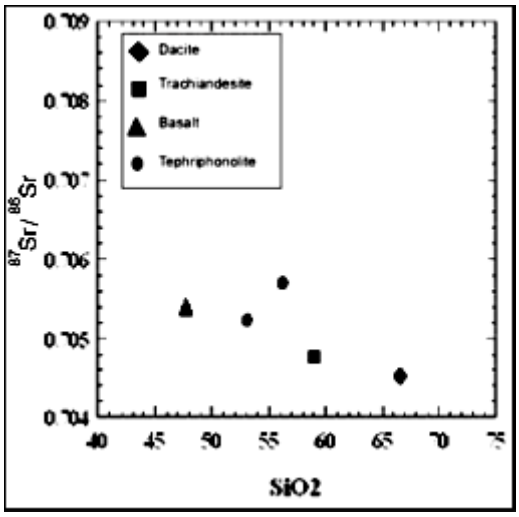

Figure 8. Plot of $^{87}Sr/^{86}Sr$ versus SiO_2 for samples from Nadik.

crystallization of primary analcite phenocrysts at depth, followed by rapid vertical transport and quenching at the surface. Pirsson [52], Gupta and Fyfe [26], Taylor and Mackenzie [60], and Wilkinson [65] interpreted the presence of analcite in the Crowsnest volcanics to replacement of primary leucite by analcite through a process of ion exchange with Na-rich fluids.

Karlsson and Clayton [2,30] found that the analcites in the volcanic rocks have either exchanged oxygen with external fluids at subsolidus temperatures or were formed from a preexisting mineral such as leucite. They favored the latter hypothesis based upon the absence of primary hydrous igneous minerals. Tephriphonolite rocks from Nadik area contain brown-white megascopic crystals of euhedra analcite of up to 5 Cm in diameter. The total amount of analcite in these rocks can locally be as high as 35Vol%, that often show multiple twin lamellae in thin section, similar to those of leucite (Fig. 2). This indicates that it has replaced primary leucite phenocrysts.

The analcite phenocrysts are fresh, and commonly contain primary inclusion of other mineral phases, particularly apatite, Fe-Ti oxides, pyroxene and feldspar. In the Nadik area the analcite clearly originated by pseudomorphous replacement of a precursor which had a euhedral trapezohedral crystal form. In addition, the high modal content of the pseudomorphous analcite trapezohedra requires that the precursor is a common mineral in undersaturated alkali-rich potassic volcanic rocks. On the basis of the trapezohedra crystal form and occurrence in rocks of this type, potential precursor is leucite.

Although garnet is reasonably common in igneous rocks, particularly alkaline types, where Ti-rich andradite (melanite) is developed [11], it is a very unlikely precursor for the analcite crystals. Melanite garnet is unaltered and shows no evidence of resorption in phonolites from the Crowsnest formation of Alberta. Garnet if developed would also be stable at the Nadik area. The whole-rock geochemistry of the tephriphonolite from Nadik also precludes the former occurrence of appreciable Ti-garnet. Ti is generally considered to be relatively immobile during the alteration [63]. The low TiO_2 contents (Table 5) of the Nadik tephriphonolites are inconsistent with the former occurrence of significant amount of any Ti-bearing phase.

Because many of the data relevant to consideration of leucite as being the precursor mineral also impinge on the origin of the large analcite trapezohedra, these two potential precursors will be considered concurrently. Leucite and its alteration products comprising analcite, nepheline, alkali feldspar, muscovite and carbonates, commonly occur in undersaturated, K-rich volcanic rocks [20].

The most spectacular crystals consist of large euhedral trapezohedra now composed of analcite but which are interpreted as having originated by pseudomorphous replacement of leucite. The origin of small analcite trapezohedra which occur in igneous rocks in veins, cavities and as replacement of glass is widely accepted as being due to low grade metamorphism or hydrothermal processes, but the large crystals have been interpreted both as primary phases which have crystallized from a silicate melt and as pseudomorphous after leucite formed by ion-exchange reaction.

Analcitization of leucite is a common geologic phenomenon [26,65], caused significant increases in the Na/K ratios of tephriphonolite. Also euhedral analcite crystals in igneous rocks are now generally explained as low-temperature alteration products of leucite, nepheline, or other precursor minerals. The major arguments based on petrography, geochemistry and experimental data both for and against the primary origin of these large crystals have been presented and discussed by Karlsson and Clayton [29,30] and Pearce [48,49]. A major feature in support of a secondary origin of large analcite crystals in igneous rocks is the very restricted, high range of pressure (5-12 Kbar P_{H2O}) and temperature (600°C-660°C) for analcite stability in simplified synthetic systems [31]. In addition, the transformation of leucite to analcite has been demonstrated experimentally and proceeds very rapidly at a subsolidus temperature either during cooling [60] or after host magma solidification [26]. The conversion of leucite to analcite that resulted from two-way diffusion involving Na^+, H_2O and K^+ across the original leucite-glass interfaces and probably was largely accomplished during hydrothermal hydration of the vitric groundmass [65].

The absence of hydrous primary igneous minerals such as amphibole or mica in the analcite-rich lavas from the Nadik area indicates that the magma was not H_2O saturated, suggesting that the formation of analcite from leucite is a more viable explanation than the igneous analcite hypothesis [31]. Also, lack of evidences for rapid transport of crystals from the depths indicated by the stability field for analcite. In addition, primary crystallization of a Na-rich phase such as analcite would necessitate crystallization of a sodic pyroxene rather than diopside.

The possibility of leucite to analcite transformation in the Nadik is likely because of petrographic evidence and preponderance of K_2O over Na_2O in bulk rock composition similar to that suggested by Church, [6]. The homogenous nature of the large, single crystals of analcite is also more consistent with a secondary origin

rather than formation by magmatic crystallization [32]. The large analcite trapezohedra are interpreted as having formed by ion-exchange pseudomorphous replacement of primary leucite either during cooling or shortly afterwards. The ease, rapidity and selectivity of the replacement process are evidenced by the lack of effect on the other phases included in analcite.

Potassium contents are less than maximum of 2 Wt%, K_2O indicated for igneous analcite from experimental studies. However, albitization of sanidine is an indication of Na mobilization and is consistent with the leucite-analcite transformation at the same time [30].

In comparison to those of the rift volcanic rocks, most of the potassic rocks from the Nadik show high Al_2O_3, K_2O, LFSE and LREE abundances and low abundances of TiO_2 and HFSE (Ta, Nb and Zr), In addition to LREE>Nb and Zr>y (Tables 5 and 6). These features provide strong evidence of the involvement of subduction-related processes in the generation of orogenic potassic magma in the Nadik area. Also, trace element ratios suggest a subduction zone source for the Nadik lavas. Values for La/Nb (2.3-3.3), La/Th (2.5-3.0) and Ba/La (277.9-62.2) are all within the range defined by orogenic volcanic [23]. Figures 9 and 10 (Zr Vs Nb and TiO_2 Vs Al_2O_3) show that all samples from the studied plot within the subduction field. Isotopic ($^{87}Sr/^{86}Sr$ and $^{143}Nd/^{144}Nd$) and geochemical evidence of this study are similar to those obtained by Hassanzdeh [28] from the Miduk area and in shoshonitic rocks from Gourougou center [24]. Relatively low $^{87}Sr/^{86}Sr$ (0.704273-0.705668) values and high $^{143}Nd/^{144}Nd$ values for Nadik volcanic rocks (Tables 5 and 6), are related to the subducted oceanic crust and the mantle wedge above the subducted slab, and / or combination of these two endmember sources. However, tephriphonolite and trachyandesite with a strong LREE enrichment but a much flatter HREE patterns from Nadik area compared with modeling results of suggestive of a spinel lherzolite source [13]. It is proposed that the positive ϵNd values (+1.3 to+ 4.1), low TiO_2, Y and HREE abundances characteristic of Nadik rocks are due to derivation of magmas from depleted zone of uppermost mantle. However, many observed geochemical variations in Nadik rocks, particularly in $^{87}Sr/^{86}Sr$ ratios, Ba, LREE and scatter incompatible elements reflect heterogeneity in the mantle source for the Nadik rocks [59].

Conclusions

The Eocene volcanic rocks from the Nadik area are composed of tephriphonolite, basalt, trachybasalt, trachyandesite and dacite. These rocks have common mineralogical characteristics. The exception is the tephriphonolite which contains abundant up to 35% of large trapezohedra of analcite.

All samples are porphyritic with a holocrystalline groundmass. The mineralogy of most samples from the Nadik area comprises analcite, sanidine, plagioclase, pyroxene, hornblende, biotite, olivine and titano-magnetite. Sanidine is the only K-feldspar present in tephriphonolite and trachyandesite. Also, diopside is the only pyroxene presented in samples from Nadik area. Based on the IUGS recommendation, these extrusive rocks are subdivided into tephriphonolite, basalt, trachybasalt, trachyandesite and dacite. There are some significant geochemical differences among the volcanic

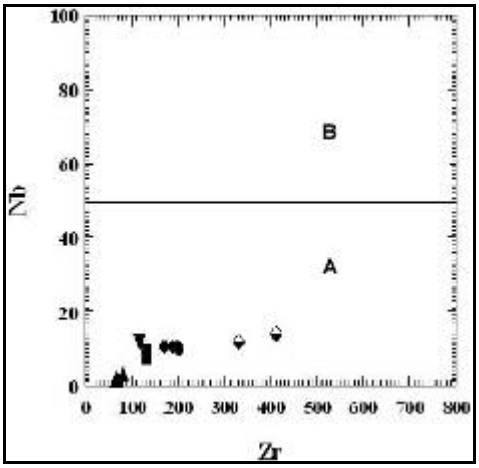

Figure 9. Zr versus Nb for potassic rocks from the Nadik after Thorpe, [62]. A=Subduction related. B=within-plate(rift related).

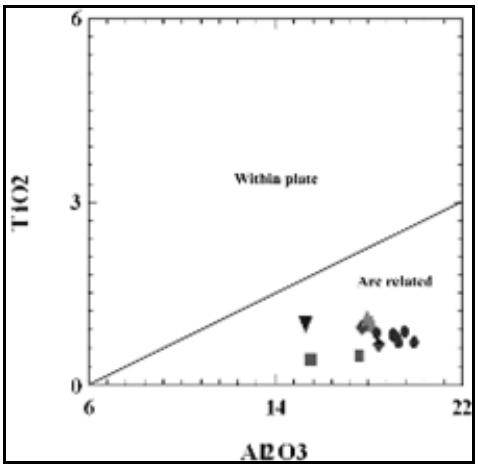

Figure 10. Al_2O_3 versus TiO_2 for potassic rocks from the Nadik, after Muller & Grovers [43].

rocks from Nadik area, particularly in the abundances of alkalies and the degree of silica saturation. However, there are some similarities including low Mg-numbers, TiO_2 and compatible elements, high contents of Al_2O_3, CaO and the incompatible elements Sr, Rb, Th, Nd and LREE. These rocks are strongly fractionated in LREE and have a flat MREE to HREE pattern with moderate to strong negative Eu anomalies.

The Tertiary rocks from Nadik have initial $^{87}Sr/^{86}Sr$ ratios between 0.70453 and 0.70567 and the ϵNd values range from +1.3 to +4.1. The samples of tephriphonolite have the highest initial $^{87}Sr/^{86}Sr$ ratio, and the lowest ϵNd (+1.3) compared with other samples from the Nadik area. Due to negative correlation of Sr isotopic value from mafic to felsic rocks of the Nadik region, these rocks can not be genetically related.

All tephriphonolite rocks from Nadik area contain brown-white trapezohedra of euhedra analcite and up to 5 Cm in diameter. Based on the following evidences the large analcite trapezohedra from the Nadik area are interpreted as having formed by ion-exchange pseudomorphous replacement of primary leucite either during cooling or shortly afterwards.

1. The samples show multiple twin lamellae in thin section similar to those of leucite.

2. The absence of hydrous primary igneous mineral such as amphibole or mica in the analcite-rich lavas from the Nadik area.

3. Lack of evidence for rapid transport of crystals from the depths indicated by the stability field for analcite.

4. Primary crystallization of a Na-rich phase such as analcite would necessitate crystallization of a sodic pyroxene rather than diopside.

5. Preponderance of K_2O over Na_2O in bulk rock composition, also K_2O and Fe_2O_3 contents of the Nadik analcite are very low.

6. The homogenous nature of the large, single crystals of analcite is also more consistent with a secondary hydrothermal origin rather than formation by magmatic crystallization.

7. The ease, rapidity and selectivity of the replacement process are evidenced by the lack of effect on the other phases included in analcite.

Most of the potassic rocks from the Nadik show high Al_2O_3, K_2O, LFSE and LREE abundances and low abundances of TiO_2 and HFSE (Ta, Nb and Zr), in addition to LREE >Nb and Zr >Y. These features provide strong evidence of the involvement of subduction-related processes in the generation of orogenic analcite-bearing potassic magma in the Nadik area.

Acknowledgements

Financial support for field work and chemical analyses was provided by Shahid Bahonar University of Kerman. I would like to express my special thanks and deep appreciation to Prof. A. Aftabi and Dr. H. Ahmadipour (Shahid Bahonar University of Kerman) for their help, guidance and encouragement throughout this research.

I wish to thanks Bruce Chappell and David Granett for assistance during the analytical work at the Australian National University and Bequerel Laboratories.

References

1. Amidi S.M. Contribution a letude stratigraphique, petrologique et petrochimique des roches magmatiques de la region Natanz-Nain Surk (Iran central). *Thesis*, universite scientifique et medicale de Grenoble, France (unpubl) (1975).
2. Berberian F. and Berberian M. Tectono-plutonic episodes in Iran. In: Gupta H.K. and Delany F.M. (Eds.), *Zagros, Hindu Kush, Himalaya Geodynamic Evolution*, pp. 5-32, American Geophysical Union Geodynamics Series 3 (1981).
3. Berberian F., Muir I.D., Pankhurst R.J., and Berberian M. Late Cretaceous and Early Miocene Andean-type plutonic activity in northern Makran and Central Iran. *Journal of the Geological Society of London*, **139**: 605-614 (1982).
4. Bubnova R.S., Stepanov N.K., Levin A.A,. Filatiov S.K., Paufler P., and Meyer D.C. Crystal structure and thermal behaviour of boropollucite CsBSi2O6. *Solid State Sciences*, **6**: 626-637 (2004).
5. Chappell B.W. Geochemical and isotopic systematics in carbonatites and implications for the evolution of ocean-island sources. *Geochimica et Cosmochimica Acta*, **52**(1): 1-17 (1988)
6. Church B.N. Shackanite and related Analcite-bearing lavas in British Colombia. *Canadian Journal of Earth Science*, **15**: 1669-1672 (1978).
7. Comin-Chiaramonti P., Meriani S., Mosca R., and Sinigoi S. On the occurrence of analcite in the northeastern Azerbaijan volcanics (northwestern Iran). *Lithos*, **12**: 187-198 (1979).
8. Coombs D.S. X-ray observations on wairakite and non-eubie analcime. *Min. Mag.*, **30**: p. 699 (1955).
9. Cundari A. Petrogenesis of leucite-bearing lavas in the Roman Volcanic Region, Italy. The Sabatini lavas. *Contributions to Mineralogy and Petrology*, **70**: 9-21 (1979).
10. Deer W.A., Howie R.A., and Zussman J. *Rock Forming Minerals*. Vol. 4, framework Silicates, 2nd Ed., Longman, Essex (1975).
11. Deer W.A., Howie R.A., and Zussman J. *Rock-forming Minerals*. Volume 1A, 2nd Ed., Orthosilicates, Longman, London (1982).
12. Dimitrijeovic M.D. Geology of Kerman region. Geological Survey of Iran, Yu/52: 334 p. (1973).
13. Dingwell D.B. and Brearley M. Mineral chemistry of

igneous melanite garnets from analcite-bearing volcanic rocks, Alberta, Canada. *Contributions to Mineralogy and Petrology*, **90**: 29-35 (1985).
14. Dostal J. and Muller W. Archean shoshonites from the Abitib Greenstone Belt Chibougamau (Quebec, Canada): Geochemistry and tectonic setting. *Journal of Volcanology and Geothermal Research*, **53**: 145-165 (1992).
15. Dostal J., Breitsprecher K., Church B.N., Thorkelson D., and Hamiton T.S., Eocene melting of Precambrian lithospheric mantel: Analcite-bearing volcanic rocks from the Challis-Kamloops belt of south central British Columbia. *Ibid.*, 303-326 (2003).
16. Dupuy C., Michard A., Dostal J., Dautel D., and Baragar W.R.A. Isotope and trace-element geochemistry of Proterozoic Natkusiak flood basalts from the northwestern Canadian Shield. *Chemical Geology*, **120**: 15-25 (1995).
17. Ellam R.M. and Harmon R.S. Oxygen isotope constraints on the crustal contribution to the subduction related magmatism of the Aeolian islands, Southern Italy. *Journal of Volcanology and Geothermal Research*, **44**: 105-122 (1990).
18. Embey-Isztin A., Downes H., James D.E., Upton B.G.J., Dobosi G., Ingram G.A., Harmon R.S., and Scharbert H.G. The petrogenesis of Pliocene alkaline volcanic rocks from the Pannonian Basin, eastern Central Europe. *Journal of Petrology*, **34**: 317-343 (1993).
19. Ferguson L.J. and Edgar A.D. The petrogenesis and origin of the analcite in volcanic rocks of the Crowsnest Formation, Alberta. *Canadian Journal of Earth Sciences*, **18**: 69-77 (1978).
20. Fiton J.G. and Upton B.G.J. *Alkaline Igneous Rocks*. Blackwell Sci. Pub., 568 p. (1987).
21. Ghasemi A. and Talbot C.J. A new tectonic for Sanandaj-Sirjan Zone (Italy). *Journal of Asian Earth Sciences*, pp. 11 (2005).
22. Giampaolo C. and Lombardi G. The thermal behaviour of Analcites from tow different genetic environment. European journal of mineralogy **6**(2): 285-289 (1994).
23. Gill J.B. *Orogenic Andesites and Plate Tectonics*. Springer-Verlag, Berlin (1981).
24. Gill R.C.O., Aparicio A., EL Azzouzi M., Hernandez J., Thirlwall M.F., Bourgois J., and Marriner G.F. Depleted arc volcanism in the Alboran Sea and shoshonitic volcanism in Morocco: geochemical and isotopic constraints on Neogene tectonic processes. Lithos **78**: 363-388 (2004).
25. Green T.H. Experimental studies of trace element partitioning applicable to igneous petrogenesis-Sendona 16 years later. *Chemical Geology*, **117**: 1-36 (1994).
26. Gupta A.K. and Fyfe W.S. Leucite survival: The alteration to analcite. *Canadian Mineralogist*, **13**: 361-363 (1975).
27. Hanson G.N. Rare earth elements in petrogenetic studies of igneous systems. *Annual Review of Earth and Planetary Sciences*, **8**: 371-406 (1980).
28. Hassanzadeh J. Metallogenic and tectonomagmatic events in the SE sector of the Cainozoic active continental margin of Central Iran (Shahrbabak area, Kerman Province). *Ph.D. Thesis*, University of California, Los Angeles (unpubl.) (1993).
29. Henderson C.M.B. and Giib F.G.F. Formation of analcite in the Dippin Sill, Isle af Arran. *Mineralogycal Magazine*, **41**: 534-537 (1977).
30. Karlsson H.R. and Clayton R.N. Analcite phenocrysts in igneous rocks: Primary or secondary reply. *American Mineralogist*, **78**: 230-232 (1993).
31. Karlsson H.R. and Clayton R.N. Analcite phenocrysts in igneous rocks: Primary or secondary. *Ibid.*, **76**: 189-199 (1991).
32. Karlsson H.R. and Clayton R.N. Oxygen and hydrogen isotope geochemistry of zeolites. *Geochimica et Cosmochimica Acta*, **54**: 1369-1386 (1990b).
33. Kim K.T. and Burley B.J. Phase equilibria in the system Na-AlSi5O8-NaAlsiO4-H2O with special emphasis on the stability of analcite. *Canada Journal of Earth Sciences*, **8**: 311-337 (1971).
34. Lambert R.St.J. and Holland J.G. Yttrium geochemistry applied to petrogenesis utilising calcium-yttrium relationships in minerals and rocks. *Geochimica et Cosmochimica Acta*, **38**: 1393-1414 (1974).
35. Le Maitre R.W., Bateman P., Dudek A., Keller J., Lameyre Le Bas M.J., Sabine P.A., Schmid R., Soresenlt,. Streekeisen A., Wooley A.A.R., and Zanettin B. *A Classification of Igneous Rocks and Glossary Terms*. Blackwell, Oxford (1989).
36. Lescuyer J.L. and Riou R. Geologie de region (Azerbaijan), contribution a letude du volcanisme tertiare de l Iran., *Ph.D. Thesis*, Grenoble University Grenolble, France, 232 p. (1976).
37. Lotfi M. Petrology and petrography study of igneous rocks, Northeast Minab, Iran. *M.Sc. Thesis*, University of Tehran, Tehran (unpubl.) (1974).
38. Line C.M.B., Putnis A., Putnis C., and Giampaolo C. The dehydration kinetics and microtexture of analcite from two paragenesis. *American Mineralogist*, **80**: 268-279 (1995).
39. Luhr J.F. and Kyser T.K. Primary igneous analcite: The Colima minettes. *American Mineralogists* (1989).
40. McBirney A.R. Effects of assimilation. In: Yoder H.S. (Ed.), *The Evolution of the Igneous Rocks*, pp. 307-338, Princeton University press, Princeton, New Jersey (1979).
41. McCulloch M.T. The role of subducted slabs in an evolving Earth. *Earth and Planetary Science Letters*, **115**: 89-100 (1993).
42. Moradian A., Petrological study of feldespathoid rocks, Javazm Shahrbabak, Iran. *M.Sc. Thesis*, University of Tehran, Tehran (unpubl) (1991).
43. Muller D. and Groves D.I. *Potassic Igneous and Associated Gold-Cupper Mineralization*. Soringer, 241 pp. (1997).
44. Nelson D.R. Isotopic characteristics of potassic rocks: Evidence for the involvement of subducted sediments in magma genesis. *Lithos*, **28**: 403-420 (1992).
45. Norish K. and Chappell, B.W. X-ray fluorescence spectrometry. In: Zussman J. (Ed.), *Physical Methods in Determinative Mineralogy*, 2nd Ed., pp. 201-272, Academic Press, London (1977).
46. Paukov I.E., Belitsky I.A., and Fursenko B.A. Heat capacity and thermodynamic functions of leucite at low temperatures. *Thermochemica Acta*, **387**: 23-28 (2002).

47. Pearce T.H. and Kolisnik A.M. Observations of plagioclase zoning using interference imaging. *Earth Science Reviews*, **29**: 9-26 (1990).
48. Pearce T.H. The analcite-bearing volcanic rocks of the Crowsnest Formation, Alberta. *Canadian Journal of Earth Sciences*, **7**: 46-66 (1970).
49. Pearce T.H. Analcite phenocrysts in igneous rocks: Primary or secondary, discussion. *American Mineralogist*, **78**: 225-229 (1993).
50. Perini G., Tepley III F.J., Davidson J.P., and Conticelli S. The origin of K-feldspar megacrysts hosted in alkaline potassic rocks from central Italy: a track for low-pressure processes in mafic magmas. *Lithos*, **66**: 223-240 (2002)
51. Petters T.J., Luth W.C., and Tuttle O.F., The melting of analcite solid solution in the system NaAlSiO4-NaAlSi3O8-H2O. *American Mineralogists*, **31**: 736-753 (1966).
52. Pirsson L.V., Scientific intelligence, II, geology and mineralogy 4, the Crownest volcanics. *American Journal of Science*, **39**: 222, 223 (1915).
53. Rickwood P.C. Boundary lines within petrologic diagrams which use oxides of major and minor elements. *Lithos*, **22**: 333-344 (1989).
54. Saha P. The system NaAlSiO2, (nepheline)-NaAlSi3O8 (albite)-H2O. *American Mineralogist*, **46**: 859-884 (1961).
55. Sardic A., Dimitrijevic M.N., Omaljer V., and Radovanovic Z. The geological map of Anar 1:100,000 sheet. Geological Survey of Iran (1972).
56. Seymour K.St. and Vlassopoulos D. Magma mixing at Nisyros volcano, as inferred from incompatible trace-element systematics. *Journal of Volcanology and Geothermal Research*, **50**: 273-299 (1992).
57. Singer B.S., Dungan M.A., and Layne G.D. Textures and Sr, Ba, Mg, Fe, K, and Ti compositional profiles in volcanic plagioclase: Clues to the dynamics of calcalkaline magma chambers. *American Mineralogist*, **80**: 776-798 (1995).
58. Stalder P. Magmatisem tertiare et subrecent enter Taleghan et Alamout, Elborz central (Iran). Bull, Suisse de min, et petrol. V.51/1, 138 p. (1971).
59. Stolz A.J., Varne R., Davies G.R., Wheller G.E., and Foden J.D. Magma source components in an arc-continent collision zone: The Flores-Lembata sector, Sunda arc, Indonesia. *Contributions to Mineralogy and Petrology*, **105**: 585-601 (1990).
60. Taylor D. and Mackenzie W.S. A contribution to the pseudoleucite problem. *Ibid.*, **49**: 321-333 (1975).
61. Thompson R.N., Gibson S.A., Leat P.T., Mitchell J.G., Morrison M.A., Hendry G.L., and Dickin A.P. Early Miocene continental extension-related basaltic magmatism at Walton Peak, northwest Colorado: Further evidence on continental basalt genesis. *Journal of the Geological Society of London*, **150**: 277-292 (1993).
62. Thorpe R.S. Permian k- rich volcanic rocks of Devon: Petrogenesise, tectonic setting and geological significance. *Transactions of the Royal Society of Edindurgh, Earth Sciences*, **77**: 361-364 (1987).
63. Van Baalen M.R. Titanium mobility in metamorphic systems: a reviw. *Chemical Geology*, **110**: 233-249 (1993).
64. Washington H.S. The analcite basalt Sardinia. *Jeournal of Geology*, **22**: 742-753 (1914).
65. Wilkinson J.F.G. Analcite phenocrysts in a vitrophyric analcimite-primary of secondary. *Contributions to Mineralogy and Petrology*, **64**: 1-10 (1977).
66. Williams H., Turner F.J., and Gilbert C.M. Petrography: *An Introduction to the Study of Rocks in Thin Sections*, 2nd Ed., 626 p. W.H. Freeman, San Francisco (1982).
67. Woolley A.R. and Symes R.F. The analcite-phyric phonolites (blairmorites) and associated analcite kenytes of the Lupate gorge, Mozambique. *Lithos*, **9**: 9-15 (1976).